



Trade Science Inc.

ISSN : 0974 - 7486

Volume 9 Issue 1

Materials Science

An Indian Journal

Full Paper

MSAIJ, 9(1), 2013 [8-23]

Optical properties of poly (vinyl alcohol)/hydroxypropyl cellulose blends

Osiris W.Guirguis*, Manal T.H.Moselhey

Biophysics Department, Faculty of Science, Cairo University, Giza, (EGYPT)

E-mail : osiris_wgr@yahoo.com

Received: 25th April, 2012; Accepted: 5th October, 2012

ABSTRACT

Transparent films of poly (vinyl alcohol)/hydroxypropyl cellulose (PVA/HPC) blend with different concentrations were prepared by using solution-cast technique. Variations in the group coordination in the IR region were followed. The effects of HPC concentrations on the optical characterizations of the films have been done by analyzing the absorbance, transmittance and reflectance spectra in the spectral region 200–2500 nm. The study has been extended to include the changes in the optical parameters including the band tail width and band gap energies for the samples. Moreover, the extinction coefficient (k) has been calculated for the investigated films. As obtained by the FTIR and NIR results, the increase in the concentration of HPC with PVA changed the chemical bonds and hence changed the molecular configuration of PVA. The results indicate that the optical band gap was derived from Tauc's extrapolation and decreases with the HPC contents. ©2013 Trade Science Inc. - INDIA

KEYWORDS

Poly (vinyl alcohol);
Hydroxypropyl cellulose;
FTIR technique;
Near infrared analysis;
Extinction coefficient;
Optical parameters.

INTRODUCTION

The term “biomaterial” has been defined as “a non-viable material used in a medical device intended to interact with biological systems”. The categories of materials that are used as biomaterials include metals, ceramics, carbons, glasses, modified natural biomolecules, synthetic polymers and composites consisting of various combinations of these material types^[1].

The physical properties of polymers may be affected by doping; the certain structural, optical, mechanical, electrical and magnetic properties of the selected polymer can be controllably modified owing to the type of the doping, concentration, and the way in which it pen-

etrates and interacts with the chains of the polymer. Detailed studies of doped polymer with different dopant concentrations allow the possibility of choice of the desired properties^[2].

PVA is unique among polymers (chemical compounds made up of large, multiple-unit molecules) in that it is not built up in polymerization reactions from single-unit precursor molecules known as monomers. Instead, PVA is made by dissolving another polymer, polyvinyl acetate (PVAc), in an alcohol such as methanol and treating it with an alkaline catalyst such as sodium hydroxide. The resulting hydrolysis, or “alcoholysis,” reaction removes the acetate groups from the PVAc molecules without disrupting their long-chain structure.

The chemical structure of the resulting vinyl alcohol repeating units is^[3]: $(-[-CH_2-CHOH-]_n-)$. When the reaction is allowed to proceed to completion, the product is highly soluble in water and insoluble in practically all organic solvents. Incomplete removal of the acetate groups yields resins less soluble in water and more soluble in certain organic liquids. The physical and chemical properties of PVA depend to a great extent on its method of preparation.

Poly (vinyl alcohol) (PVA), a colorless, water-soluble synthetic resin employed principally in the treating of textiles and paper. PVA is used in sizing agents that give greater strength to textile yarns and make paper more resistant to oils and greases. It is also employed as a component of adhesives and emulsifiers, as a water-soluble protective film, and as a starting material for the preparation of other resins.

PVA was selected as the hydrogel component based on its favorable water-soluble, desirable physicochemical properties and its biocompatibility^[4]. Furthermore, chemically crosslinked PVA hydrogel has been gaining increasing attention in the field of biomedics^[5].

A graft copolymer is a type of branched copolymer with the side chain being different and separate from the main chain. As in the case of the graft copolymer, the copolymer formed usually combines the properties of both polymers which forms the copolymer^[6].

The amalgamation of polymer and pharmaceutical sciences led to the introduction of polymer in the design and development of drug delivery systems. Polysaccharides fabricated into hydrophilic matrices remain popular biomaterials for controlled-release dosage forms and the most abundant naturally occurring biopolymer is cellulose; so hydroxypropylmethyl cellulose, hydroxypropyl cellulose, microcrystalline cellulose and hydroxyethyl cellulose can be used for production of time controlled delivery systems. Targeting of drugs to the colon following oral administration has also been accomplished by using polysaccharides such as hydroxypropyl cellulose in hydrated form^[7].

Hydroxypropyl cellulose (HPC) belongs to the group of cellulose ethers which has been used already for a year by paper of conservators as glue and sizing material. The material is soluble in water as well as in polar organic solvents (makes it possible to combine aqueous and non aqueous conservation methods)^[8].

HPC is used as a topical ophthalmic protectant and lubricant^[9]; as a food additive; a thickener and as an emulsion stabilizer with E number E463. In pharmaceuticals HPC used as a disintegrants and a binder for the wet granulation method of making tablets^[10-13].

In the present study, a trail will be carried out to produce the best product of poly (vinyl alcohol)/hydroxypropyl cellulose blend and also to overcome the defects of the individual homopolymers. FTIR techniques were employed to characterize and reveal the miscibility map and the structure properties of such blending system. Furthermore, the present work concerned with the investigation of the effect of different concentrations of HPC on the optical properties of poly (vinyl alcohol) films, by performing UV/VIS/NIR analysis which gives an evidence for understanding energy band diagram and optical parameters which is relatively affected by processing conditions.

EXPERIMENTAL

Materials and sample preparation

Poly (vinyl alcohol) (PVA) granules with molecular weight of 125 kg/mole was supplied from El-Nasr Company, Cairo, Egypt. Hydroxypropyl cellulose (HPC; Pharmacoat 606) with molecular weight of 95 kg/mole was supplied by Shin Etsu Chemical Co., Tokyo, Japan.

The solution method^[14-16] was used to obtain film samples. This method depends on the dissolution, separately, the weighted amounts of the poly (vinyl alcohol) (PVA) granules and hydroxypropyl cellulose (HPC) powder in double distilled water. Complete dissolution was obtained using a magnetic stirrer in a 50 °C water bath. To prepare thin films of the homopolymers (PVA and HPC) and the blend of their samples (PVA/HPC) with different weight percentages 100/0, 90/10, 75/25, 50/50, 25/75 and 0/100 wt/wt%, the solutions were mixed together at 50 °C with a magnetic stirrer. Thin films of appropriate thickness (about 0.01 cm) were cast onto stainless steel Petri dishes (10 cm diameter). The prepared films were kept at room temperature (ca. 25 °C) for 7 days until the solvent completely evaporated and then kept in desiccators containing fused calcium chloride to avoid moisture. The samples were

Full Paper

measured at room temperature (about 25 °C) as solid films (slabs) of dimensions 1 x 4 cm.

Fourier transform infrared (FTIR) spectroscopy

The Fourier transform infrared absorption (FTIR) spectra of the samples under investigations were performed over the range 4000-400 cm^{-1} using a Bruker Vector 22 Spectrophotometer (Germany) with accuracy better than $\pm 1\%$.

UV/VIS/NIR spectroscopic measurements

The measurements in the ultraviolet region from 200 to 400 nm, visible region from 400 to 700 nm and NIR region from 900 to 2500 nm for pure PVA, HPC and PVA/HPC blended samples were carried out using a Shimadzu (UV/VIS/NIR) Double Beam Spectrophotometer with standard illuminant C (1174.83) and has a serial number B44360512, Model V-530 and band width 2.0 nm covers the range 200-2500 nm with accuracy $\pm 0.05\%$.

RESULTS AND DISCUSSIONS

Fourier transform infrared (FTIR) spectral analysis

It is well known that IR spectroscopy can be used to detect the existence of specific interaction in polymer and blends and also reflects the specific groups which are found in all components. Moreover, FTIR spectroscopy has long been recognized as a powerful tool for elucidation of structural information. The position, intensity, and shape of vibrational bands are useful in clarifying conformational and environmental changes of polymers at the molecular level^[17].

Figure 1 shows the FTIR absorbance spectra for PVA/HPC blended samples as functions of wavenumber in the range 4000-600 cm^{-1} . The chemical assignments were considered and are shown in TABLE 1. The spectrum of PVA seems to be consistent with that previously reported in the literatures^[18,19]. Amorphous and crystalline phases show partly resolved absorption in the 1150-1000 cm^{-1} region. The chemical assignments for PVA, HPC and their blended samples were considered and are also illustrated in TABLE 1.

It is clear from the figure and the table for PVA (curve a) that a relatively broad and intense ν (OH)

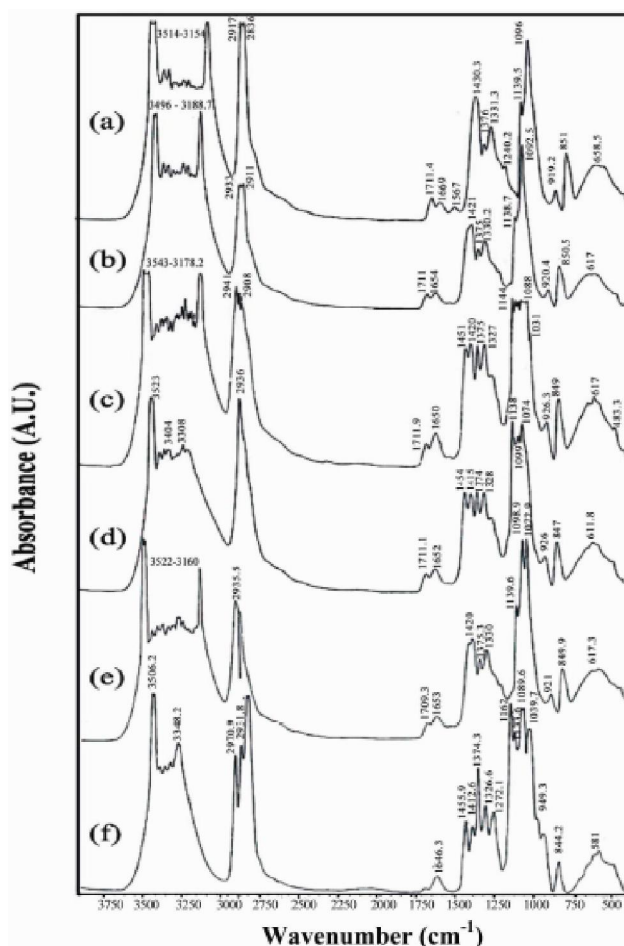


Figure 1 : Variations in FTIR spectra of PVA/HPC blended samples: (a) 100/0, (b) 90/10, (c) 75/25, (d) 50/50, (e) 25/75 and (f) 0/100 (wt/wt%).

absorption stretching band is observed between 3515-3154 cm^{-1} indicating the presence of a polymeric association of the free hydroxyl group and bonded OH stretching vibration^[20,21]. This broad and intense band usually occurs along with sharp less intense “monomeric” and “dimeric” OH absorption. Also, two distinct absorption bands occurring at 2936 and 2918 cm^{-1} result from antisymmetric ν_{as} (CH_2) and symmetric ν_{s} (CH_2) stretching vibrations, respectively.

The bands at 1712 and 1567 cm^{-1} of the carbonyl group are due to absorption of the residual acetate group^[3]. The band at 1712 cm^{-1} was assigned to ‘free’ unassociated and to associated hydrogen-bonded carbonyl group in the sample^[21]. The band at 1659 cm^{-1} was attributed to the absorption of H_2O ^[22]. The symmetric bending mode ν_{s} (CH_2) is found at 1430 cm^{-1} . In addition, the bands at 1376 and 1240 cm^{-1} result from rocking methyl groups (CH_3) or wagging vibra-

TABLE 1 : Positions and assignments of the most absorption bands of PVA/HPC blended samples

Wavenumber (cm ⁻¹)						Assignments
PVA/HPC blended sample (wt/wt%)						
100/0	90/10	75/25	50/50	25/75	0/100	
3515-3154	3490-3188	3543-3178	3523-3282	3544-3160	3516-3348	Hydrogen bonded and hydroxyl O-H group
2936	2933	2942	2937	2935	2971	CH ₂ or CH ₃ stretching vibration
2918	2911	2925	-	-	2911	C-H stretching vibration
-	-	2880 shoulder	2883 shoulder	2883 shoulder	2894	C-H stretching vibration
1712	1711	1712	1711	1709	1716	Carbonyl group C=O stretching
1660	1654	1651	1653	1653	1646	Water absorption and C=O stretching
1567	1566	1567	-	-	-	Carbonyl group C=O stretching
1430	1422	1421	1415	1420	1456	O-H, C-H bending and -CH ₂ deformation
-	-	-	-	-	1413	Bending vibration mode of CH ₂
1376	1376	1375	1375	1375	1374	-CH ₂ wagging
1331	1330	1327	1328	1330	1327	C-H and O-H bending
1240	1216	-	1283	1234	1272	O-H bending and C-H wagging
1140	1139	1124	1138	1140	1134	C-O stretching vibration
1096	1093	1089	1074	1099	1090	C-O stretching vibration
-	-	1031	-	-	1040	C-O stretching vibration
919	920	926	926	921	949	C-O deformation and -CH ₂ rocking
851	850	849	847	850	844	Skeletal and -CH ₂ rocking
607	617	617	611	617	617	O-H Twisting

tions of CH₂ and CH, respectively. The band at about 1331 cm⁻¹ is assigned to mixed ν_s (CH and OH) bending modes and is attributed to the associated alcohols.

The stretching band at 1140 cm⁻¹ is known to be the crystallization-sensitive band of PVA and is taken as a measure of the degree of crystallinity. It is believed that this band arises from the symmetric ν (C-C) stretching mode related to the regular repetition of the trans-configuration of the zigzag chain in a crystalline region. In addition, it is inferred that the 1140 cm⁻¹ band might be due to a kind of absorption mechanism related to the presence of the oxygen atom. The band at about 1096 cm⁻¹ is assigned to ν (C-O) stretching vibration of ether group. The band at 919 cm⁻¹ is related to syndiotactic structure and is assigned to the ν_r (CH₂) rocking vibration. The bands at 851 cm⁻¹ is assigned to -CH₂ rocking vibration and at 607 cm⁻¹ due to O-H twisting^[22].

From the obtained results for PVA/HPC blended samples shown in Figure 1 and TABLE 1, it is clear

that:

- The absorbance band observed at 3515-3154 cm⁻¹ which is due to the presence of hydrogen bonded O-H group in pure PVA sample becomes narrower by adding different concentrations of HPC.
- The strong band at 2936 cm⁻¹ associated with C-H stretching vibration of pure PVA shows little shifts in its position and decrease in its intensity by adding different concentrations of HPC.
- The band at 1712 cm⁻¹ associated with carbonyl group (C=O) of pure PVA shows little shifts in its position and intensity by adding of different concentrations of HPC.
- The band at 1659 cm⁻¹ associated with water absorption and C=O stretching shows shift in its position and its intensity decreases with increasing HPC concentration.
- The band at 1567 cm⁻¹ associated with carbonyl group C=O shows little shift in its position and decrease in its intensity by increasing HPC concen-

Full Paper

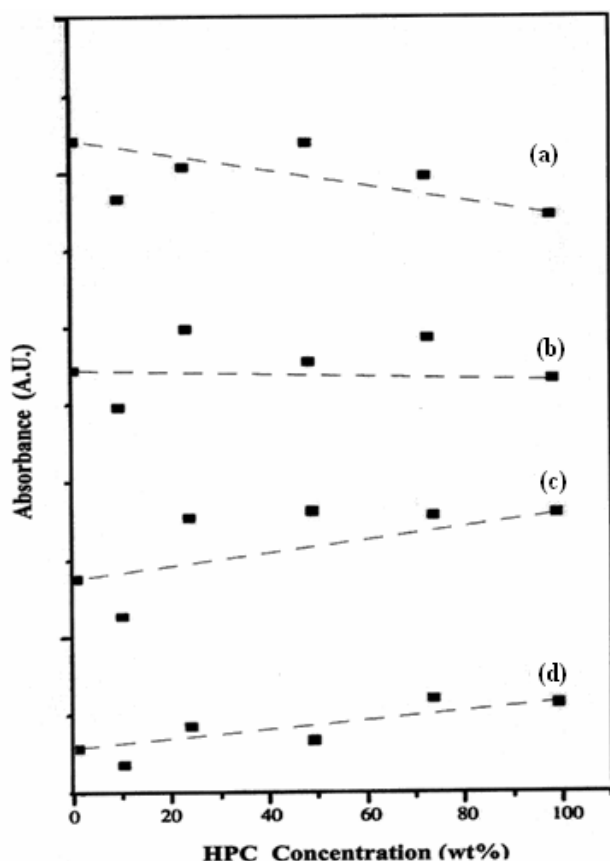


Figure 2 : Variation in band intensities for some chemical groups of PVA/HPC blended samples as functions of HPC concentration at: (a) 2942-2932 cm^{-1} , (b) 1331-1327 cm^{-1} , (c) 1144-1134 cm^{-1} and (d) 949-919 cm^{-1}

tration (10 and 25wt% HPC), then disappeared completely for 50/50 and 25/75 wt/wt% PVA/HPC blended samples.

- The band at 1430 cm^{-1} associated with O-H bending and CH, CH₂ deformation shows shift in its position and decrease in its intensity by adding different concentrations of HPC.
- The bands at 1376 and 1331 cm^{-1} associated with CH₂ wagging and C-H or O-H bending show unremarkable shift in their positions and intensities by adding of HPC concentration.
- The bands at 1140, 1096 and 851 cm^{-1} associated with C-O stretching vibration, skeletal and CH₂ rocking, respectively show nearly unremarkable shift in their positions.

By following the FTIR spectra, it is easily assigned the observed strong band as OH-stretching vibration. The variation of this band intensity with increasing HPC contents may have allowed us to specify a strong or

weak interaction between HPC ions and the O-H stretching groups belonging to different chains in PVA^[14,15]. The presence of hydrogen-bonded structures in some polymers could be inferred at once from the presence of the bond form of the hydrogen stretching mode. Thus, in PVA, the OH band at 3514-3154 cm^{-1} showed that the molecular chains formed hydrogen bonds. The FTIR spectra shown in Figure 1 were completely absorbed in the OH-stretching for all the samples. Moreover, O-H groups are polar groups, and the accessibility for polar groups is of great importance in polymer modification (especially in fabrication). The position and the bonding of these groups are influenced by crystallinity and crystal modification. Furthermore, the increase in absorbance of carbonyl groups indicates decrease in their growth, which may suggest that they are converted into volatile compounds^[21]. A decrease in carbonyl groups can be related to enhancement of some mechanical properties of the polymers. The shape of the carbonyl band at 1712 cm^{-1} indicated a change in the balance of free and associated carbonyl groups in the blends. The hydroxyl and carbonyl stretching vibration bands are affected by hydrogen bonding interactions and are most amenable to quantitative analysis.

The heights of the peaks of the assigned groups at their wavenumbers shown in the spectra were taken to represent the variation in the group band intensities for different HPC concentrations (Figure 2). A clear deviation was observed in the absorption bands of the PVA/HPC copolymers when compared with that detected for pure PVA. Any increase or decrease means a change in the molecular configuration of the polymer.

As shown by the FTIR results, it was clear that an increase in the concentration of HPC changed the chemical bonds and hence changed the molecular configuration of PVA which is shown by the pronounced variation in the intensity of absorbance bands and little shifts in band positions. The change in intensity and disappearance of some spectral bands associated with infrared active groups of the polymer (PVA and HPC) may be attributed to the fact that in the polymeric materials that contain two or more components, the resulting spectrum is approximately the sum of there components. In addition, the change in the spectral position of some bands of PVA after the additions of different HPC concentrations may be attributed to some of the

monomer units of PVA are sensitive to their environment. Also, the frequency shifts of the bands due to the HPC for the samples of the blends imply that there is a specific interaction between HPC and PVA^[17]. Shifts in bands positions in the spectra of the copolymer are observed as opposed to homopolymers^[22].

It is known that the type of bonding in the network structure plays a dominant role in deciding the rigidity of the structure and also associated with the change in cross-linkage and coordination of the polymer network^[23].

The stretching force constant (F) in Newton and the local bond length in nm were also calculated from the following equations:

$$F = [2\pi c \nu]^2 \cdot \mu \quad (1)$$

Where c is the speed of light, ν is the frequency in Hz and μ is the reduced mass given by:

$$\mu = [(Z_a/N_A) \cdot (Z_b/N_A)] / [(Z_a/N_A) + (Z_b/N_A)] \quad (2)$$

Where N_A is the Avogadro's number, Z_a and Z_b are the atomic number of the atoms respectively which form the bond. In case of double bond, equation (2) is divided by 2. Therefore, the bond length is given by^[24,25]

$$\text{Bond length} = \{(X_a \cdot X_b)^{3/4} / [(F-30)/(5.28 \cdot O)]\}^{2/3} \quad (3)$$

Where X_a and X_b are the electronegativity of the atoms, respectively, which share in the bond length, O is the bond order (for single bond $O = 1$, while for double bond $O = 2$) and F is the stretching force.

TABLE 2 shows the stretching force and the bond length for the effective band frequencies of O-H, C-H, C=O and CH_2 of PVA/HPC blended samples. It is noticed that there are changes in both stretching force and bond length. The presence of hydrogen in bonded structures in some polymers can be inferred at once from the presence of the bond-form of the hydrogen stretching mode. It is clear from the table in calculation of bond length that^[24]:

- Hydroxyl O-H group decreased as the concentration increases which indicated that increase in elastic moduli.
- C=O stretching group bond length increases as the concentration increases which means that the elastic moduli decreases by increasing the concentration.
- C-H bending group remains the same by increasing the concentration.

- For -CH_2 rocking group the bond length decreased as the concentration increased which indicated that increase in elastic moduli.

Near infrared (NIR) spectral analyses

The absorbance spectra and the assignments of the most important absorbance bands in the near infrared region (900-2500 nm) for PVA/HPC blended samples are shown in Figure 3. TABLE 3 illustrates the variation of the peak position while TABLE 4 represents the change in the area of each peak, the band width and the absorbance values of some bands as well as the bond vibration and structure for PVA/HPC blended

TABLE 2 : The stretching force and the bond length for PVA/HPC blended samples

Blend sample PVA/HPC (wt/wt%)	Wavenumber (cm^{-1})	Reducing mass (kg)	Stretching force (N)	Bond length (nm)
Hydroxyl (O-H) group				
100/0	3334	1.57×10^{-27}	620.5	0.119
90/10	3340	1.57×10^{-27}	6225	0.118
75/25	3361	1.57×10^{-27}	630.36	0.117
50/50	3403	1.57×10^{-27}	646.34	0.115
25/75	3352	1.57×10^{-27}	627.28	0.118
0/100	3432	1.57×10^{-27}	657.48	0.114
C=O stretching group				
100/0	1660	1.14×10^{-26}	556.06	0.218
90/10	1654	1.14×10^{-26}	552.64	0.2197
75/25	1651	1.14×10^{-26}	550.19	0.220
50/50	1653	1.14×10^{-26}	551.42	0.220
25/75	1653	1.14×10^{-26}	551.68	0.2199
0/100	1646	1.14×10^{-26}	547.21	0.221
C-H bending group				
100/0	1430	1.54×10^{-27}	111.97	0.380
90/10	1422	1.54×10^{-27}	110.65	0.384
75/25	1421	1.54×10^{-27}	110.46	0.385
50/50	1415	1.54×10^{-27}	109.63	0.388
25/75	1420	1.54×10^{-27}	110.42	0.385
0/100	1413	1.54×10^{-27}	109.21	0.389
Skeletal and -CH_2 rocking group				
100/0	919	1.54×10^{-27}	92.49	0.456
90/10	920	1.54×10^{-27}	92.74	0.454
75/25	926	1.54×10^{-27}	93.93	0.449
50/50	926	1.54×10^{-27}	93.87	0.449
25/75	921	1.54×10^{-27}	92.86	0.454
0/100	949	1.54×10^{-27}	98.64	0.428

Full Paper

samples. It is noticed from Figure 3 and TABLE 3 for PVA/HPC blended samples that^[26]:

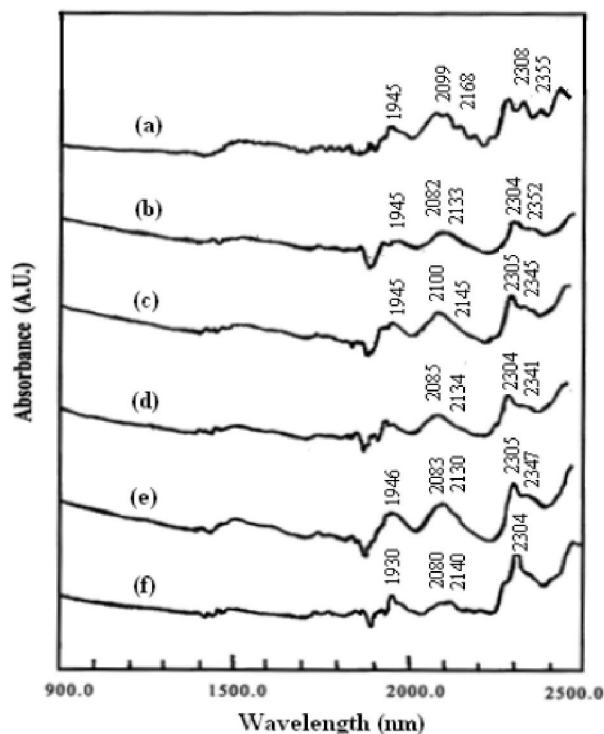


Figure 3 : Variation in NIR spectra of PVA/HPC blended samples: (a) 100/0, (b) 90/10, (c) 75/25, (d) 50/50, (e) 25/75 and (f) 0/100 (wt/wt%)

- The bands at 2410 nm for pure PVA and at 2472 nm for pure HPC are disappeared in all doped concentrations.
- The band at 2352 nm appeared only in pure PVA and 10 wt% HPC and then shifted towards lower wavelength (2345 nm) with increasing the HPC concentration.
- Disappearance of band at 2200 nm for pure PVA and at 2197 nm for pure HPC.
- Band at 1945 nm shifted toward lower wavelengths by increasing HPC concentration up to 50 wt% (at about 1930 nm) as the pure HPC sample.
- The band at 1898 nm for pure HPC shifted toward higher wavelengths by doping HPC with PVA.
- The band at 1780 nm for pure PVA disappeared by doping HPC in all doped concentrations.
- The band at 1764 nm for pure HPC shifted toward lower values of wavelengths by adding HPC with different concentrations and appeared at around 1752 nm.
- The bands at 1724 nm for pure PVA and at 1732 nm for pure HPC disappeared and observed at about 1713 nm by doping PVA with different concentrations of HPC.

From TABLE 4 of PVA/HPC blended samples, it

TABLE 3 : Positions and assignments of the most NIR absorption bands of PVA/HPC blended samples

Wavelength (nm)	PVA/HPC blended sample (wt/wt%)						Assignment	Chemical Structure
	100/0	90/10	75/25	50/50	25/75	0/100		
2410	—	—	—	—	—	2472	C-H stretching + C-C stretching	= CH group
2355	2352	—	—	—	—	—	C-H deformation-second overtone	HC=CHCH ₂
—	—	2345	2341	2347	—	—	CH ₂ sym. Str. + CH ₂ deformation	
2308	2304	2305	2304	2305	2304	2304	C-H stretching + C-H deformation	CH ₂ or CH ₃
2208	—	—	—	—	—	2197	C-H stretching + C = O stretching	- CHO
2168	2133	2145	2134	2130	2140	2140	=C-H stretching + C=O stretching	- CHO
2099	2082	2100	2085	2083	2080	2080	O-H stretching + O-H deformation	ROH
1945	1945	1945	—	1946	1930	1930	O-H stretching + O-H deformation	H ₂ O
—	1908	1906	1898	1871	1898	1898	C=O str. Secondary overtone	-(O ₂ H)
1815	1810	1830	1820	1818	1820	1820	O-H stretching + 2(C-O) stretching	Cellulose
1780	—	—	—	—	—	—	C-H stretching first overtone	Cellulose
1752	1753	—	1751	1751	1764	1764	C-H stretching first overtone	CH ₂
1724	1713	1713	1714	1713	1732	1732	C- H stretching first overtone	CH ₃ or CH ₂

TABLE 4 : Variation of the peak position, the area under the peak and the band width for PVA/HPC blended samples

Blend sample PVA/HPC	Peak Position	Area under the peak	Band width (nm)	Absorbance	Assignment	Chemical structure
For 2310 nm						
100/0	2308	5.119	0.4	0.4477	C-H stretching + C-H deformation	CH ₂ or CH ₃
90/10	2304	2.039	0.4	0.3865		
75/25	2305	4.157	0.5	0.5365		
50/50	2304	3.211	0.4	0.4454		
25/50	2305	4.307	0.4	0.6370		
0/100	2304	5.423	0.4	0.4365		
For 2133 nm						
100/0	2168	1.148	0.4	0.3387	=C-H stretching + C=O stretching	-CHO
90/10	2133	2.957	0.15	0.3827		
75/25	2145	3.156	0.7	0.4510		
50/50	2134	2.530	0.17	0.3650		
25/50	2130	5.248	1.6	0.5493		
0/100	2140	3.264	0.4	0.0069		
For 2090 nm						
100/0	2099	10.787	0.9	0.3972	O-H stretching + O-H deformation	ROH
90/10	2082	2.911	0.7	0.3568		
75/25	2100	3.572	0.7	0.4879		
50/50	2085	3.196	0.7	0.3852		
25/50	2083	4.374	0.7	0.5802		
0/100	2080	2.399	0.8	0.2936		
For 1940 nm						
100/0	1945	4.367	0.7	0.3464	O-H stretching + O-H deformation	H ₂ O
90/10	1945	3.409	0.3	0.3304		
75/25	1945	5.698	0.8	0.4607		
50/50	—	2.211	0.3	0.3749		
25/50	1946	7.592	0.8	0.5547		
0/100	1930	3.366	0.4	0.3182		

is clear that:

- At the peak position 2310 nm of CH₂ or CH₃ group that: the behavior is a fluctuation behavior and when the area decreases the intensity of the peak decreases and vice versa.
- At the peak position 2133 nm for -CHO group: as the concentration of HPC increases the area increases and so the intensity of the peak increases.
- At the peak position 2090 nm for ROH group: the area under the peak sharply decreased with increasing the concentration of HPC toward the pure HPC value.
- At the peak positions 1940 nm for H₂O group: the behavior is a fluctuated behavior.

Moreover, the variation in the intensity of the peaks means that there are changed in the molecular configuration as the dopant concentration changed. A clear variation was observed in the peak positions, and peak

areas of the PVA/HPC copolymers when compared with that shown for the homopolymers samples. In addition, it is noticed that strong local interaction between HPC and other groups belonging to different chains in PVA will take place at the expense of the intermolecular interaction between these chains. This in turn can be directly correlated with variations in the mechanical behavior of the polymer^[27]

Electronic absorption (UV/VIS) analyses

The study of optical absorption spectra provides essential information about the band structure and the energy gap in crystalline and non-crystalline materials. Analysis of the absorption spectra in the lower energy part gives information about atomic vibrations, while the higher energy part of the spectrum gives knowledge about electronic state in atoms. Hence, the study of optical properties in the UV/VIS regions can help in

Full Paper

a better understanding of the electronic structure and optical material constants^[28,29].

Figure 4 shows the absorption spectra of PVA/HPC blended samples with different concentrations of HPC (10, 25, 50 and 75 wt%) in the wavelength range 200-700 nm. It is clear from the figure that the curves are closed to each other in the visible region (400-700 nm). Sharp drops in the absorbance values were detected in

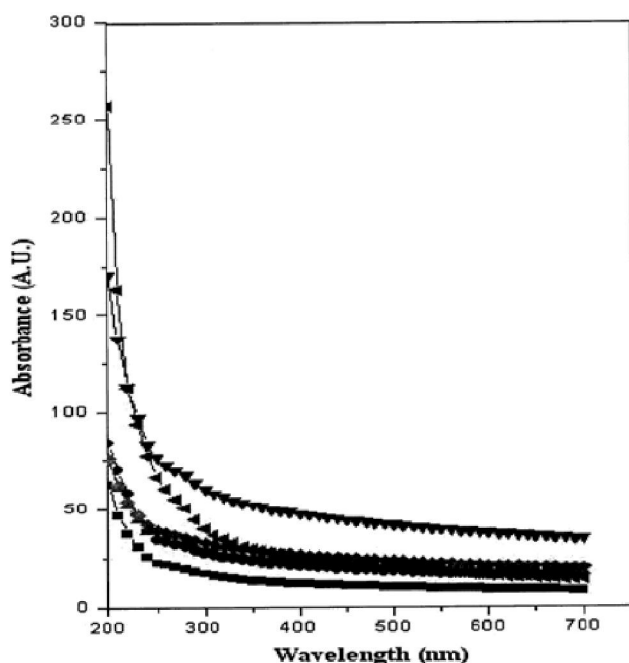


Figure 4 : The absorption spectra of PVA/HPC blended samples: (■) 100/0, (●) 90/10, (▲) 75/25, (▼) 50/50, (◆) 25/75 and (◄) 0/100 (wt/wt%)

the UV region (200-400 nm). The spectrum of pure PVA exhibits a shoulder like band at 280 nm which are related to high energy absorption. This band is assigned to the existence of carbonyl groups associated with ethylenic unstauration of the type $[-(C=C)_n-C=O]$, $n = 2, 3$ ^[29]. The carbonyl groups may arise from charge-transfer reactions during polymerization with acetaldehyde, a hydrolysis of vinyl acetate or with the decomposition products a vinyl acetate-oxygen copolymer.

The variation in the absorbance values of the blended samples with increasing the concentration of HPC may be attributed to the fact that increasing the dopant concentration decreases the transparency of the sample which may be due to that there is a change in the molecular configuration^[30]. The spectra are composed of an almost flat baseline and a step cutoff (big absorption). The absorbance values for homopolymers (PVA

and HPC) are lower than those for blend compositions through the wavelength range 200-700 nm.

Optical parameters of PVA, HPC and their blends

The absorption coefficient (α) of the present mate-

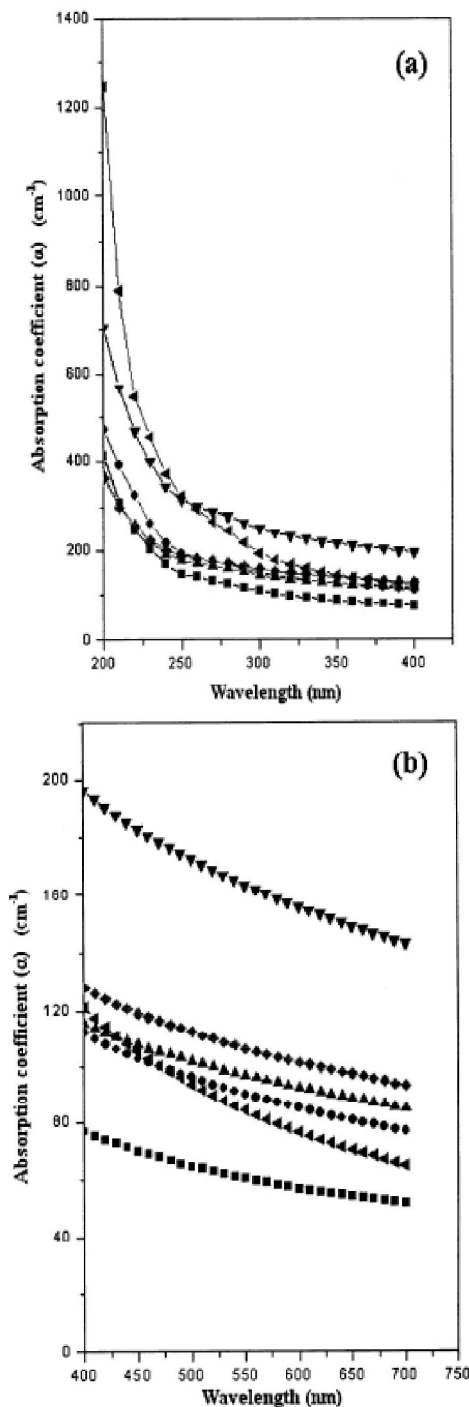


Figure 5 : The absorption coefficient (α) of PVA/HPC blended samples as a function of wavelengths in the UV range 200-400 nm (a) and in the visible range 400-700 nm (b): (■) 100/0, (●) 90/10, (▲) 75/25, (▼) 50/50, (◆) 25/75 and (◄) 0/100 (wt/wt%)

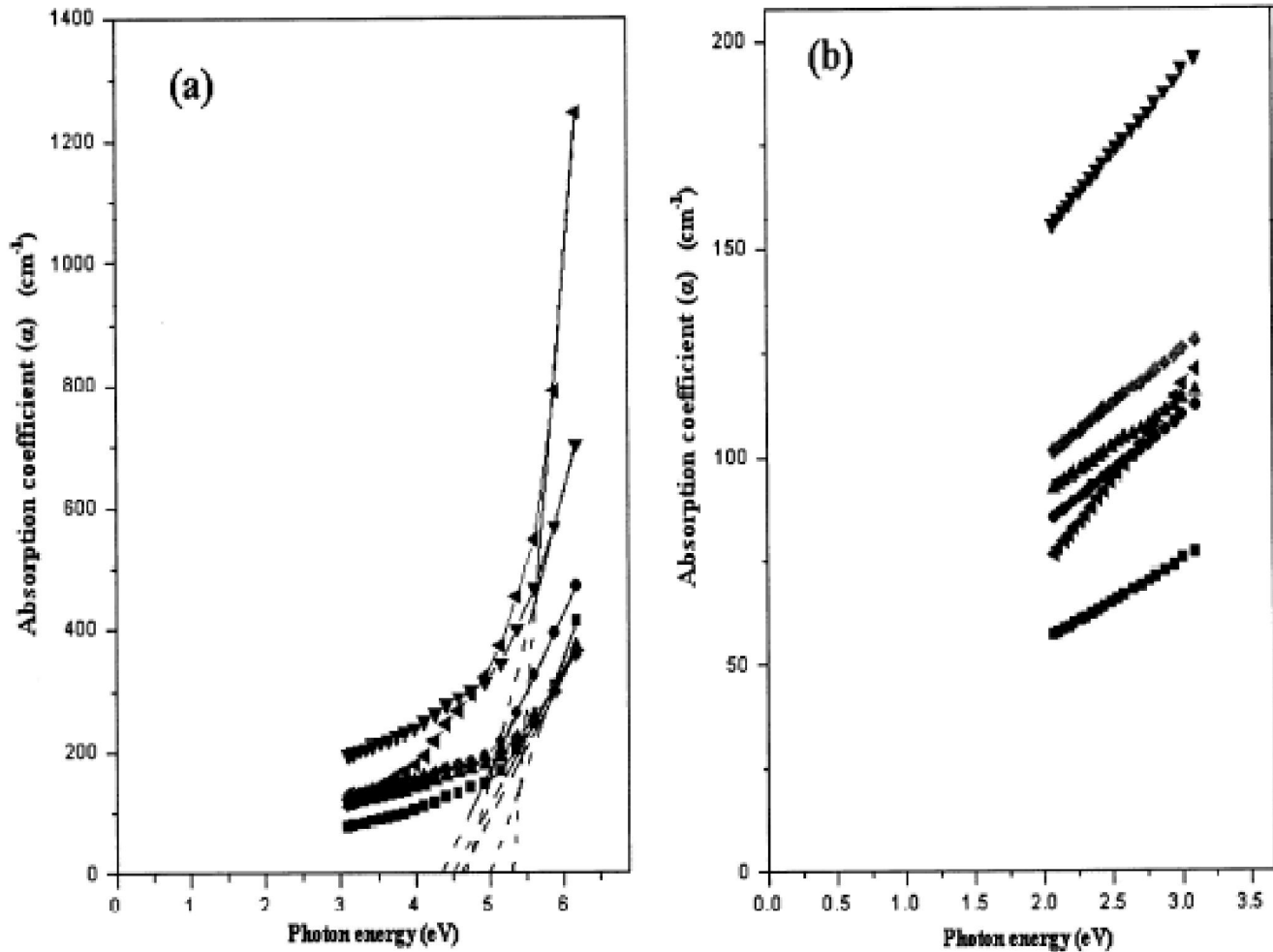


Figure 6 : The absorption coefficient (α) of PVA/HPC blend samples as a function of photon energy ($h\nu$) in the UV range 3.0-6.5 eV (a) and in the visible range 2.0-3.2 eV (b): (■) 100/0, (●) 90/10, (▲) 75/25, (▼) 50/50, (◆) 25/75 and (◄) 0/100 (wt/wt%)

rials strongly depends on optical transmission (T), reflection (R) and thickness of film (d) which is evaluated using the relation^[31,32]:

$$\alpha = [\ln(1-R)/T]^2 / d \quad (4)$$

Where T is the transmittance and d is the thickness of the sample in cm (the reflectance, R is neglected in this calculation).

The total absorption spectral response (α) for PVA, HPC homopolymers and their blends were calculated in the (UV/VIS) wavelength range from 200 to 700 nm and in the photon ranges 3.0-6.5 eV (UV-region) and 2.0-3.2 eV (VIS-region).

Figure 5 shows the relation between the absorption coefficient (α) as a function of wavelength in the UV range 200-400 nm (a) and in the visible range 400-700 nm (b) for PVA/HPC blended samples. It is clear from the figures that the absorption coefficient increases

gradually with increasing HPC concentration but it decreases at concentration 75 wt% HPC. The increase in α with the increase in the HPC concentration up to 50 wt%, which is the highest one, may be attributed to the change of the molecular configuration which leads to the formation of new color centers^[14,15].

The fundamental absorption edge is one of the most important features of the absorption spectra of crystalline and amorphous materials. The increased absorption near the edge is caused by the transition of electrons from the valence band to the conduction band^[30].

Figure 6 illustrates the plot of absorption coefficient (α) against photon energy ($h\nu$) for PVA/HPC blended samples in the ranges 3.0-6.5 eV (a) and 2.0-3.2 eV (b). It is clear that, the absorption coefficient (α) increases with increasing photon energy and exhibits a steep rise near the absorption edge and a straight

Full Paper

TABLE 5 : Values of absorption edge (E_c), band tail energy (E_b), direct energy gap (E_d), and indirect energy gap (E_{ind}) for PVA/HPC blended samples

(a) In UV region (200-400 nm):				
Blended sample PVA/HPC (wt/wt%)	E_c (eV)	E_b (eV)	E_d (eV)	E_{ind} (eV)
0/0	5.00	0.368	5.09	4.25
90/10	4.32	0.305	4.68	3.50
75/25	4.50	0.242	4.51	3.55
50/50	4.64	0.264	4.54	3.75
25/75	4.68	0.213	5.25	3.59
0/100	5.36	0.546	5.73	4.82

(b) In the visible region (400-700 nm):		
Blended sample PVA/HPC (wt/wt%)	E_b (eV)	E_d (eV)
100/0	0.314	2.10
90/10	0.313	2.06
75/25	0.257	2.04
50/50	0.263	1.98
25/75	0.262	2.00
0/100	0.514	2.28

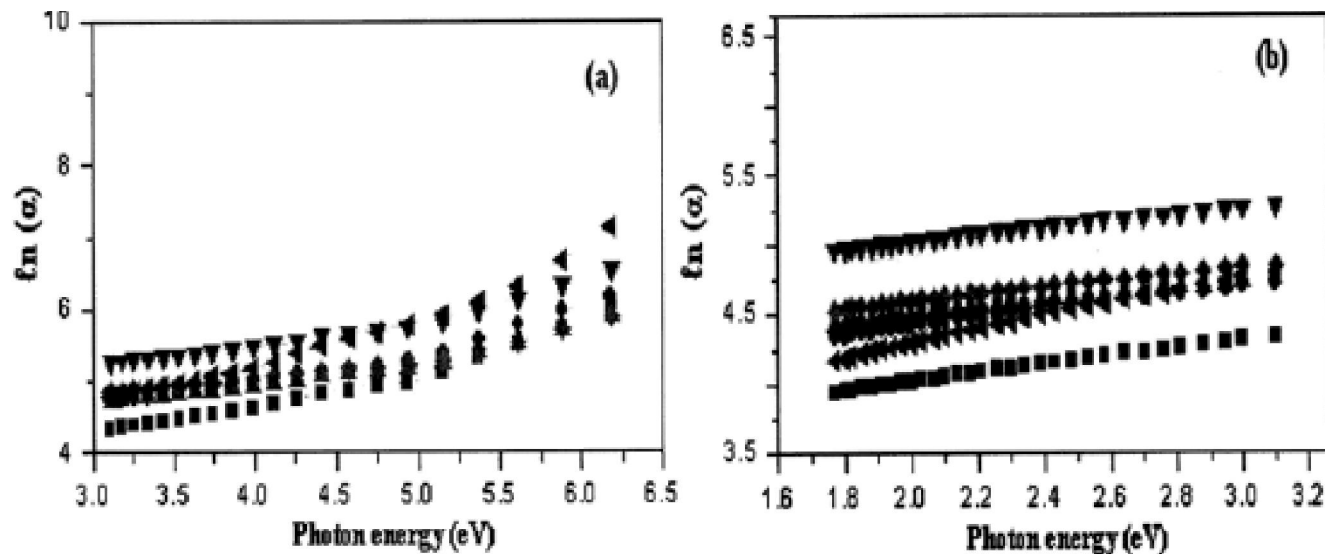


Figure 7 : Urbach law plots for PVA/HPC blended samples in the UV range (a) and visible range (b): (■) 100/0, (●) 90/10, (▲) 75/25, (▼) 50/50, (◆) 25/75 and (◄) 0/100 (wt/wt%).

line relationship is observed in the high α -region only in the 3.0-6.5 eV (UV region) (Figure 6a). The intercept of extrapolation to the straight part to zero absorption (i.e., $\alpha = 0$) with photon energy axis was taken as the value of absorption edge (E_c). The values obtained for E_c are listed in TABLE 5. It is clear that the values of the absorption edge (E_c) for the blend samples are lower than those for PVA and HPC. This may reflect the in-

duced changes in the number of available final states according to the blend composition.

The optical energy gap (E_g) of the thin films has been determined from absorption coefficient data as a function of photon energy. According to the generally accepted model proposed by Wood and Tauc^[33] for higher values of absorption coefficient where the absorption is associated with interband transitions, it yields the power part which obeys the relation^[33,34]:

$$\alpha h\nu = B (h\nu - E_g)^n \quad (5)$$

Where B is the slope of the Tauc edge called the band tail parameter and n is the type of electronic transition responsible for absorption, being 0.5 for direct transition and 2 for indirect one.

The slope of the absorption edge characterizes the width of the localized states which in turn indicates the ordering of the structure. In the low absorption region the absorption coefficient (α) shows an exponential dependence on phonon energy ($h\nu$) and obeys the Urbach

relation^[31].

$$\alpha = \alpha_0 \exp (h\nu / E_b) \quad (6)$$

Where α_0 is a constant and E_b is the Urbach energy, interpreted as the width of the tails of localized states in the band gap. Figure 7 shows the relation between $-\ln \alpha$ and $h\nu$ for PVA/HPC blended samples in the UV range 3.0-6.5 eV (a) and visible range 2.0-3.2 eV (b). The straight lines obtained suggest that the absorption

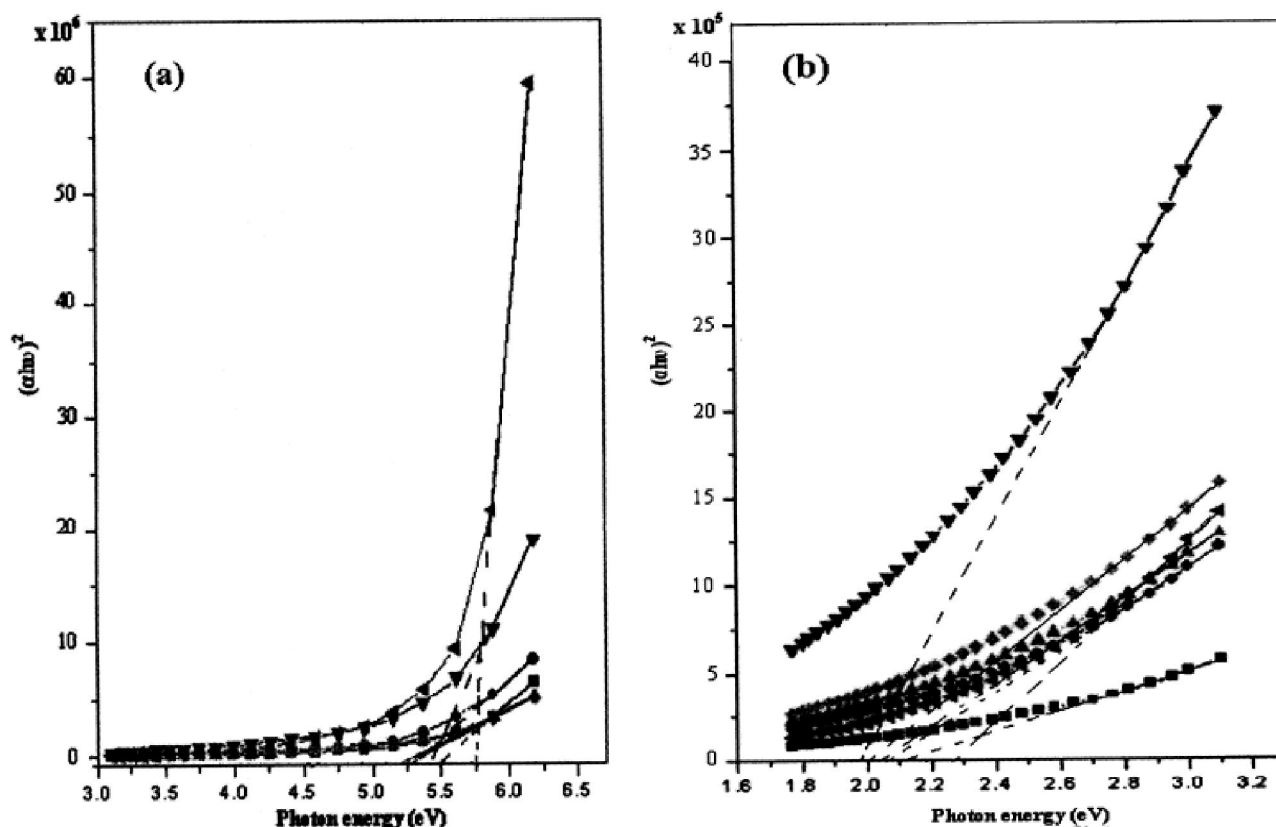


Figure 8 : The variation of $(\alpha h\nu)^2$ of PVA/HPC blended samples as a function of photon energy ($h\nu$) in the UV range 3.0-6.5 eV (a) and in the visible range 2.0-3.2 eV (b): (■) 100/0, (●) 90/10, (▲) 75/25, (▼) 50/50, (◆) 25/75 and (◄) 0/100 (wt/wt%)

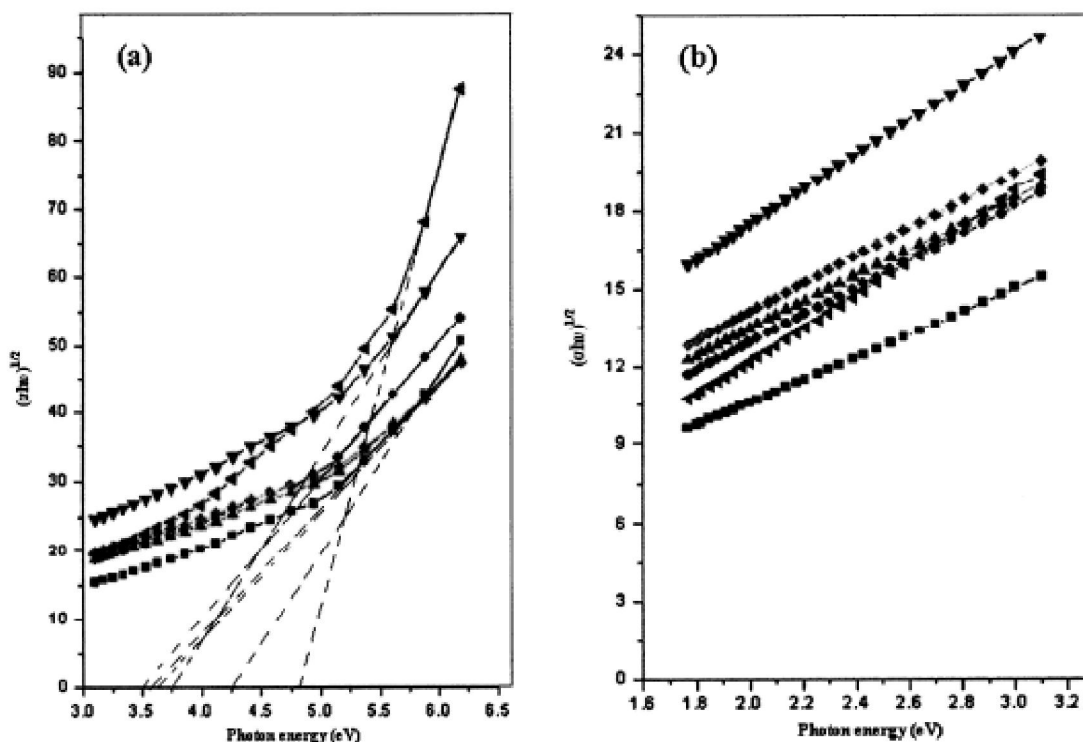


Figure 9 : The variation of $(\alpha h\nu)^{1/2}$ of PVA/HPC blended samples as a function of photon energy ($h\nu$) in the UV range 3.0-6.5 eV (a) and in the visible range 2.0-3.2 eV (b): (■) 100/0, (●) 90/10, (▲) 75/25, (▼) 50/50, (◆) 25/75 and (◄) 0/100 (wt/wt%)

Full Paper

follows quadratic relation for interband transitions and the Urbach rule is obeyed^[34]. The values of band tail energy (E_b) can be deduced from the slopes of the straight lines and are listed in TABLE 5. From the table, the values of E_b decrease with increasing HPC concentration. The tail states are generated due to disorder in the system^[34]. It has been assumed that the amorphous state is a perturbed crystalline state. The formation of polymer-polymer blends is known to induce tails in the density of states by perturbing the band edge by a deformation potential, coulomb interaction and by forming localized band states^[34]. Thus the model by Wood and Tauc^[33] based on electronic transition between localized states in the band edge tails, the density of which is assumed to fall exponentially with energy, is preferable.

Figure 8 shows the variation of $(\alpha h\nu)^2$ as a function of $h\nu$ for PVA/HPC blended samples. From the figure, the allowed direct energy gap (E_d) is determined by extrapolating the linear parts of the curves to zero absorption and the values of E_d are listed in TABLE 5. It is clear from the table that, the values E_d decrease with increasing HPC concentration. In addition, the E_d values for the blended samples are nearly closed together in the ranges 5.25-5.45 eV in the UV region and 1.98–2.06 eV in the visible region but still lower than those of the pure values of PVA and HPC in both regions.

Figure 9 shows the variation of $(\alpha h\nu)^{1/2}$ as a function of $h\nu$ for PVA/HPC blended samples. From the figures, the allowed indirect energy gap (E_{ind}) is determined by extrapolating the linear parts of the curves to zero absorption and the values of E_{ind} are represented in TABLE 5 in the UV region only. It is clear that the values of E_{ind} for the blend samples are nearly closed together and lie in the range 3.5-3.75 eV and are lower than those of both of the pure PVA and HPC samples.

From the linear plots of $(\alpha h\nu)^{1/2}$ against $(h\nu)$ for these samples as shown in figure 3, the optical energy gap has been determined from the intercepts of extrapolations to zero with the photon energy axis $(\alpha h\nu)^{1/2} \rightarrow 0$ (i.e., Tauc extrapolation). From the results obtained it is seen that an increase of concentration of HPC in the system leads to a decrease in the optical band gap.

The results obtained of E_d and E_{ind} show the dependence on the composition of the sample. It may be presumed that the variation may be due to the differ-

ence in the number of HPC ions per unit length available for conduction and, in addition, the change in molecular configuration induced by dopant concentration.

It was noticed that the variation in the values of E_b , E_d and E_{ind} with increasing the concentration of HPC may be due to HPC induced structural changes in the system. In another meaning, this change can be attributed to the effect of internal potential fluctuation associated with the structural disorder^[35]. Furthermore, it was recognized that dopant plays a dominant role in morphological and microstructure changes occurring in the polymer matrix^[14,15,29].

Extinction coefficient

The extinction coefficient (K) describes the properties of the material to light of a given wavelength and indicates the amount of absorption loss when the electromagnetic wave propagates through the material, i.e. represents the damping of an EM wave inside the material. The extinction coefficient (k) is important parameters characterising photonic materials. Value of n and k can be calculated from transmission and reflection spectra using the relation^[32]:

$$K = \alpha\lambda/4\pi \quad (7)$$

Where λ is the wavelength and α is the absorption coefficient. The decrease in the extinction coefficient with

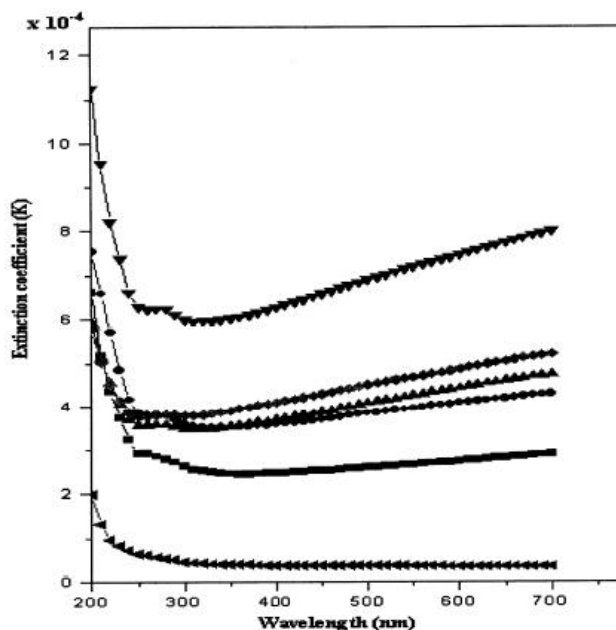


Figure 10 : Variation in the extinction coefficient (K) as a function of wavelength (λ) of PVA/HPC blended samples: (■) 100/0, (●) 90/10, (▲) 75/25, (▼) 50/50, (◆) 25/75 and (◄) 0/100 (wt/wt%)

an increase in wavelength shows that the fraction of light lost due to scattering. The decrease in K with an increase in wavelength shows that the fraction of light lost due to scattering.

Figure 10 shows the variation in the extinction coefficient (K) with wavelength of PVA/HPC blended samples. It is clear from the figure that similar behavior for all samples are observed and the values of K are found to be small in the order 10^{-4} throughout the studied wavelength range (200-700 nm) which indicate that the samples under investigation are considered to be insulating materials at room temperature^[36]. In addition, the behavior of the absorption coefficient is preserved for all samples near the absorption edge. Furthermore, it is also clear that, the blend samples 50/50 wt/wt% for PVA/HPC indicate highest values of K through the whole range of wavelength (200-700nm). Moreover, the values of K for PVA/HPC blended samples are higher than that of the PVA and HPC homopolymers' values in the whole range of wavelength.

Optical reflectance and color difference calculations of PVA/HPC blends

The relative brightness (y_r), the brightness (L), the color constants (A) and (B), the whiteness index (W), the yellowness index (Ye), the color difference (ΔE), the chroma (ΔC) and the hue (ΔH) are estimated using the CIE relations^[15,37,38].

From the values of reflectance (figures are not shown for simplicity data). TABLE 6 illustrates the values of x_r , y_r and z_r at peak positions for homopolymers and PVA/HPC blended samples. The relative brightness (y_r) is calculated and plotted as a function of wavelength (400-700 nm) and shown in Figure 11 for PVA/HPC

TABLE 6 : Represents the x_r , y_r and z_r tristimulus reflectance values of PVA/HPC blended samples calculated from reflectance data

Blended sample PVA/HPC wt/wt%	x_r		y_r	z_r
	$\lambda =$ 446.4 nm	$\lambda =$ 589.3 nm	$\lambda =$ 553.5 nm	$\lambda =$ 453.5 nm
100/0	102	217	248	526
90/10	104	217	248	526
75/25	110	233	268	575
50/50	104	217	259	538
25/75	81	167	189	408
0/100	96	202	209	450

blended samples. It is observed from the figure that, the behaviors of y_r for the samples are similar and no change in peak position (555.4 nm) is detected. It is also observed that y_r increases at HPC concentration 25 wt% and then decreases with increasing HPC concentration up to 75 wt%.

TABLE 7 represents the variation of color parameters and their percentage changes calculated from the reflectance curves for PVA/HPC blends. From the table it is observed that:

- **The brightness (L)**
The brightness (L) shows unremarkable increase with increasing the concentration of HPC.
- **The color constants A and B**
For PVA/HPC blend samples, the values of A increase by increasing the HPC concentration up to

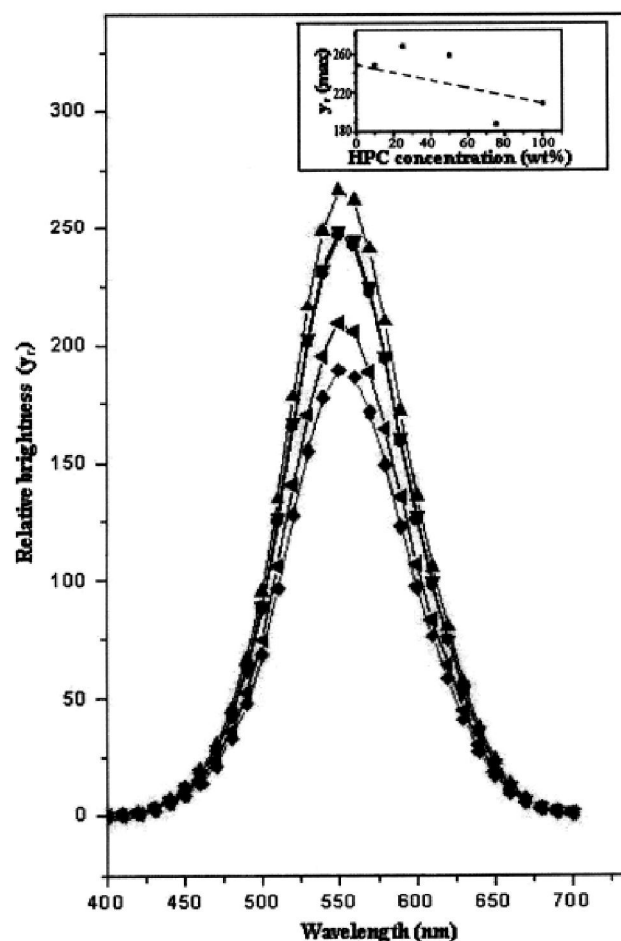


Figure 11 : Variation of the relative brightness value (y_r) with wavelength for PVA/HPC blended samples: (■) 100/0, (●) 90/10, (▲) 75/25, (▼) 50/50, (◆) 25/75 and (◄) 0/100 (wt/wt%). The inset indicates the variation y_r (max) as a function of HPC concentration.

Full Paper

75 wt% which means that there is an increase in red component instead of green one. The values of B decrease by increasing HPC concentration up to 50 wt% which indicates that there is an increase in blue component instead of yellow one and then return to the value of pure PVA at 75wt% HPC.

- **The whiteness index (W)**

The whiteness index (W) shows immeasurable change with increasing the concentration of either HPC.

- **The yellowness index (Y_e)**

The value of yellowness index (Y_e) value decreases sharply at 10 wt% HPC and then decreases with

TABLE 7 : The results of color parameters and their percentage changes for PVA/HPC blended samples calculated from the reflectance curves

Color parameters	PV A/HPC blended samples (wt/w t%)					
	100/0	90/10	75/25	50/50	25/75	0/100
L	5.5866	5.5758	5.5830	5.5812	5.5857	5.5848
ΔL%	-	-0.19	-0.06	-0.10	-0.02	-
A	0.1112	0.0962	0.1052	0.1054	0.0971	0.0987
ΔA%	-	13.49	5.40	5.22	12.68	-
B	0.1767	0.2134	0.1881	0.1969	0.1742	0.1855
ΔB%	-	-20.77	-64.52	-11.43	1.41	-
W	2.4404	2.4192	2.4336	2.4292	2.4416	0.2436
ΔW%	-	0.87	0.28	0.46	0.05%	-
Y _e	7.0891	8.0814	7.3789	7.6645	6.8109	7.1738
ΔY _e %	-	-14.00	-4.09	-8.12	3.92	-
ΔE	-	0.0411	0.0134	0.0216	0.0143	-
ΔC	-	0.0253	0.0068	0.0146	0.0096	-
ΔH	-	0.0494	0.0154	0.0267	0.0173	-

increasing HPC concentration up to 50 wt% towards the original value and then return to opposite side (-ve value) and increases for 75 wt% HPC concentration.

- The obtained results indicate that variations in color difference between samples are occurred by the presence of HPC by different concentrations with PVA.

The observed changes in the color parameters calculated from the reflectance curves with the increase in the concentration of HPC may be due to the change in the physical bonds and then changes in the molecular configuration of PVA as mentioned before which may lead to formation of new dopant centers of the polymeric material. In addition, the obtained results of the

color parameters are of great importance for the improvement of the optical properties of the PVA.

ACKNOWLEDGEMENT

The authors are very grateful to the late Prof. Dr. El-Sayed A. Gaafar, Professor of Biophysics, Biophysics Department, Faculty of Science, Cairo University, Giza, Egypt, for his kind help to bring this work.

REFERENCES

- [1] S.Dumitriu; Polymeric biomaterials, Marcel Dekker Inc., New York, (1996).
- [2] Omed Ghareb Abdullah, Sarkawt Abubakr Hussen; Variation of optical band gap width of PVA films doped with aluminum iodide, Paper presented at the international conference on manufacturing science and technology (ICMST), Kuala Lumpur, Malaysia, 26-28 November, (2010).
- [3] G.J.Prichard; Poly (vinyl alcohol): basis principles and uses, Gordon and Breach, New York, (1970).
- [4] J.Zhang, K.Yuan, Y.Wang, S.Zhang, J.Zhang; Journal of Bioactive and Compatible Polymers, **22**, 207 (2007).
- [5] S.J.Kim, Y.M.Lee, I.Y.Kim, S.I.Kim; Reactive and functional polymers, **55**, 291 (2003).
- [6] R.V.Kulkarni, B.Sa; Journal of Bioactive and Compatible Polymers, **24**, 368 (2009).
- [7] S.Kamel, N.Ali, K.Jahangir, S.M.Shah, A.A.El-Gendy; Express Polymer Letters, **2**, 758 (2008).
- [8] J.Hofenk-de Graaff; Central research laboratory for objects of art and science, Gabriel Metsustraat and 1071 EA: Amsterdam, The Netherlands, (1981).
- [9] Chandra Mohan Eaga, Jagan Mohan Kandukuri, Venkatesham Allenki, Madhusudan Rao Yamsani; Der Pharmacia Lettre, **1**, 21 (2009).
- [10] T.Ishikawa, B.Mukai, S.Shiraishi, N.Utoguchi, M.Fujii, M.Matsumoto, Y.Watanabe; Chemical & Pharmaceutical Bulletin, **49**, 134 (2001).
- [11] Chien-Yuan Leea, Gan-Lin Chenb, Ming-Thau Sheub, Cheng-Hsiung Liub; The Chinese Pharmaceutical Journal, **58**, 57 (2006).
- [12] H.H.Azita, Talasaz, A.Ali, Ghahremankhani, Shadi H.Moghadam, Mazda R.Malekshahi, Fatemeh Atyabi, Rassoul Dinarvand; Journal of Applied Polymer Science, **109**, 2369 (2008).

- [13] Suhas Nalle, Rupali Sarpate, Mallikarjuna Setty, Patan Inayat, Anand Deshmuk; Research Journal of Pharmacy and Technology, **3(1)**, (2010).
- [14] N.A.El-Zaher, W.G.Osiris; J.Appl.Polym.Sci., **96**, 1914 (2005).
- [15] Osiris W.Guirguis, Manal T.H.Moselhey; J.Mater. Sci., **46**, 5775 (2011).
- [16] Osiris W.Guirguis, Manal T.H.Moselhey; Natural Science, **4(1)**, 57 (2012).
- [17] C.S.Ha, W.K.Lee, W.J.Cho; Macromolecular Symposia, **84**, 279 (1994).
- [18] M.Shiboyama, T.Yamamoto, C.-F.Xiao, S.Sakurai, A.Hayami, S.Nomura; Polymer, **32**, 1010 (1991).
- [19] P.Sakellariou, A.Hassan, R.C.Rowe; Polymer **34**, 1240 (1993).
- [20] C.K.Park, M.J.Choi, Y.M.Lee; Polymer, **37**, 1507 (1995).
- [21] A.L.Smith; Applied Infrared Spectroscopy, Fundamentals Techniques and Analytical Problem-Solving, Wiley, New York, (1979).
- [22] R.L.Desai, J.A.Shields; Die Makromolekulare Chemie, **122**, 134 (1969).
- [23] C.Bernard, S.Chaussedent, A.Monteil, M.Montagna, L.Zampedri, M.Ferrari; Journal of Sol-Gel Science and Technology, **26**, 925 (2003).
- [24] M.S.Gaafar, S.Y.Marzouk; Physica B: Condensed Matter., **388**, 294 (2007).
- [25] Y.B.Saddeek, M.A.Azooz, S.H.Kenawy; Materials Chemistry and Physics, **94**, 213 (2005).
- [26] B.G.Osborne, T.Fearn; Near infrared spectroscopy in food analysis, Longman scientific and technical groups, John Wiley & Sons, New York, USA, (1986).
- [27] A.Tager; Physical chemistry of polymer, Mir Publishers, Moscow, Russian, (1972).
- [28] R.A.Chikwenze, M.N.Nnabuchi; Chalcogenide Letters, **7**, 389 (2010).
- [29] F.H.Abd El-Kader, S.A.Gafar, A.F.Basha, S.I.Bannan, M.A.F.Basha; Journal of Applied Polymer Science, **118**, 413 (2010).
- [30] A.Miller; Handbook of optics, McGraw-Hill, New York, USA, **1**, (1994).
- [31] M.M.Abd El-Raheem; Journal of Physics: Condensed Matter., **19**, 216209 (2007).
- [32] R.Tintu, K.Saurav, K.Sulakshna, V.P.N.Nampoori, P.Radhakrishnan, Sheemu Thomas; Journal of Non-Oxide Glasses, **2**, 167 (2010).
- [33] D.L.Wood, J.Tauc; Physical Review B., **5**, 3144 (1972).
- [34] N.F.Mott, E.A.Davis; Electronic processes in non-crystalline materials, Oxford: Clarendon, (1979).
- [35] R.M.Ahmed; International Journal of Photoenergy Article ID 150389, (2009).
- [36] J.I.Pankove, Optical process in semiconductors, Devers publication, New York, USA, (1975).
- [37] CIE recommendation on colorimetry; CIE Publ., Central Bureau of the CIE, Vienna, **15(2)**, (1986).
- [38] CIE recommendation on uniform color spaces; color difference equations, Psychometric color terms, Suppl. No. 2 of CIE Publ. (E-1.3.1), Paris, **15**, (1971,1978).